Label-free Identification of Nonelectrogenic Cancer Cells using Adhesion Noise

Maximilian Ell[1], Ralf Zeitler[2], Roland Thewes[3], Günther Zeck[1]
[1] TU Wien, Faculty of Electrical Engineering and Information Technology, Institute of Biomedical Electronics, Vienna, Austria
[2] zerodev, Stuttgart, Germany
[3] TU Berlin, Faculty of Electrical Engineering and Computer Science, Chair of Sensor and Actuator Systems, Berlin, Germany
maximilian.ell@tuwien.ac.at

***Abstract*—Time-continuous detection of cells on substrates without the need of optical microscopic imaging is of broad interest in biotechnological applications. We present a method how to detect cancer cells using voltage noise caused by cell adhesion which is recorded by high-density CMOS-based microelectrode arrays. We analyze our data in terms of spectral power density for two different types of arrays, each of them being optimized in a different working regime.**

Keywords—CMOS-based microelectrode array, cell adhesion noise, HT-29 cell.

I. Introduction

CMOS-based microelectrode arrays (CMOS MEAs) comprise several thousand densely packed sensor sites and are commonly used in biotechnological applications to record neuronal activity at high spatial (few … few tens of µm) and high temporal resolution (up to 20 kHz bandwidth). Moreover, CMOS MEAs are capable to stimulate activity with a temporal precision of few milliseconds and a spatial precision of tens of microns [1-3]. An unexplored application of CMOS MEAs is their ability to detect adherent cells by recording and analyzing the voltage noise caused by the resistive adhesion cleft [4-6]. This might be attributed to the methodology, which requires to consider the scale of the sensor site, the size of the adherent cells, the junction capacitance and the corresponding sampling frequency. Here, we therefore employ two different types of CMOS MEAs and corresponding recording systems to evaluate their ability for reliable label-free detection of an adherent cell culture (cancer cell line HT-29). Cell adhesion voltage noise from these cells is analyzed in terms of spectral power density (S_V).

Label-free detection of cells is of broad interest, for instance to determine the cells' proliferation status or transition to a cancerogenic status in a fast and cost-effective manner compared to actual molecular biology approaches, e.g., fluorescence staining or cell viability or toxicity assays. So far, electric detection of nonelectrogenic cells has only been reported using electrical impedance spectroscopy (EIS) with electrodes in the range of hundreds of microns [7], which is not suitable for single-cell detection or in the nanometer range [8], which is not suitable for the detection of cellular networks. In this work, sensing sites on the CMOS MEAs are at the scale of few microns, thus in principle allowing for very detailed maps of the adherent cells enabling both single-cell resolution and cell network studies. The cell adhesion maps calculated here are compared with ground truth light microscopic images.

II. Methods

A. Cell culture

The colorectal cancer cell line HT-29 (ATCC) is cultivated in cell culture medium (Fisher Scientific GmbH, Germany) containing 10 % v/v Fetal Bovine Serum (FBS, heat inactivated, ThermoFisher Scientific Inc., Brazil), 1 % v/v Penicillin Streptomycin (Pen Strep, Fisher Scientific GmbH, Germany) and 1 % v/v L-Glutamine 200 mM (Fisher Scientific GmbH, Germany). The cell culture medium is changed every 2 days, cells are passaged once a week.

B. Recording with CMOS MEAs

The voltage noise measurements are conducted with two different CMOS-based MEA systems. Type I MEA comes with the commercial CMOS-MEA5000 amplifier system (Multi Channel Systems MCS GmbH, Reutlingen, Germany) as described recently [9]. The MEA's sensor array provides 65 x 65 capacitive recording sites (radius a_I: 7.5 µm) with an electrode pitch of 32 µm and a total area of 2.1 mm x 2.1 mm. The top dielectric is omitted leaving the chip surface covered solely with its native TiO_2 oxide [10]. Voltage recordings are performed at 100 kHz sampling rate for 10 s using the CMOS-MEA Control software (Multi Channel Systems MCS GmbH, Reutlingen, Germany). Type II MEA (obtained from formerly Venneos GmbH, Stuttgart, Germany) offers 256 x 384 capacitive recording sites (radius a_{II}: 3.1 µm) with a pitch of 5.6 µm x 6.5 µm covering an active area of 1.6 mm x 2.5 mm as described in [11]. The top oxide (30 nm ALD-TiO_2) covers the sensor array. The voltage noise is recorded at 100 kHz sampling rate for 10 s while the spectral power density (S_V) of the voltage noise is estimated at frequencies between 1 kHz and 50 kHz using the CAN-Q Acquisition software (Venneos GmbH, Stuttgart, Germany). For chip calibration, a sinusoidal voltage (1 mVpp amplitude and 100 Hz frequency) is applied via an external Ag/AgCl electrode. This external signal defines the calibration factor that is employed to the recordings of electrode noise levels to estimate the correct data range.

A perspex culture chamber is glued on both chips such that the recording site arrays are exposed to cell culture and

medium [6]. The voltage measurements are performed either with Phosphate-Buffered Saline (PBS, Fisher Scientific GmbH, Germany) or with adherent cells in cell culture medium.

C. Interfacing cells and culturing them on CMOS MEAs

The surface of each CMOS-MEA chip is treated identically. The surface is cleaned with Tickopur R60 (5 % v/v, 80 °C, Dr. H. Stamm GmbH Chemische Fabrik, Berlin, Germany), sterilized with 70 % v/v ethanol for 15 min and rinsed with distilled water. The recording sites are covered with 50 µL of collagen (10 % v/v, Sigma Aldrich GmbH, Vienna, Austria) to ensure tight cell adhesion, incubated at room temperature for 2 h and rinsed with distilled water to remove the excessive coating solution. After cleaning and coating the chips, 100 µL of a cell-culture-medium suspension (400 cells/µL) is pipetted on top of the sensor array. The chips are incubated for one hour at 37 °C in a 5 % CO_2 atmosphere to guarantee sufficient cell sedimentation. Afterwards, the chips' chambers are filled with cell culture medium and cultivated at 37 °C and 5 % CO_2 to ensure the cells' viability. During recordings, the chips and recording hardware are placed in a safety cabinet at room temperature without additional shielding.

D. Data processing

Data processing is accomplished via customized Python scripts (Python version 3.9.5). The recorded extracellular voltages are filtered with a fourth order high pass Butterworth function at 10 Hz. The spectral power density is computed by Welch's method using the SciPy library with default settings [12].

E. Microscopy

To relate the estimated cell positions to ground truth brightfield images of the CMOS MEA's sensor array are taken using an upright light microscope (Zeiss Axioplan, 10x objective).

III. Results

The goal of the presented work is to identify cells adhered to CMOS-based MEAs using extracellular voltage noise recordings. Based on previous work with neurons [4-6], we assume that the cleft resistance between a cell and a micron-scale recording site contributes significantly to the voltage noise thus distinguishing this value from the one of a bare sensor site. The simplest way to test if cell adhesion can be detected using the extracellular voltage noise is the calculation of the root-mean-square (*rms*) noise levels. Fig. 1 demonstrates how the two systems are calibrated and shows exemplary voltage recordings. Evaluation of the average *rms* voltage noise on > 1000 sensor sites of CMOS MEA type I using PBS provides an average value of 16 µV, which is in accordance with [9]. The low voltage noise is attributed to low-noise buried channel sensing transistors. The average *rms* voltage noise of CMOS MEA type II measured under otherwise identical conditions is much higher, i.e., 70 µV. This high *rms* value can be attributed to a different CMOS process, thus different device parameters, and smaller device areas. Interestingly, the average *rms* voltage noise is not significantly different if cells adhere to the sensor sites. The average *rms* noise increases slightly to 17 µV for CMOS MEA type I and to 72 µV for CMOS MEA type II, respectively.

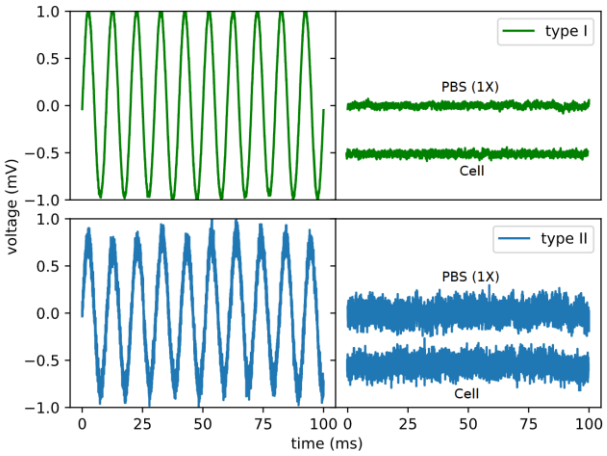

Fig. 1: Recording of an external sine wave modulation (left) and of calibrated, high-pass filtered extracellular voltage of selected sensor sites with and without adherent cells (right) using the two MEA types. The voltage traces with cells are shifted with respect to the voltage recordings with PBS for visualization purpose only. Upper row: Type I CMOS MEA [9]. Lower row: Type II CMOS MEA [11,13].

Previous studies indicate how the resistive cleft between cell membrane and planar recording site of an electrolyte-oxide-semiconductor field-effect-transistor can be estimated from the spectral power density of the voltage noise [4-6]. Nonelectrogenic cells, such as the cancer cell line HT-29, likely contribute with their resistive cleft to the adhesion noise as well. Fig. 2A exemplifies our approach for label-free identification of cells on CMOS MEAs. The spectral power density S_V is calculated in the range between 0.7 and 50 kHz for sensor sites with adherent cells and compared to the spectral power density for the same bare sensor covered with PBS. The approach is repeated for both CMOS MEAs and for two different concentrations of PBS (and thus different conductivities). Two features are extracted from the spectra: (i) an adherent cell contributes significantly to the total spectrum across the entire frequency range and (ii) low conductive medium leads to S_V values which are larger than the respective values with cells.

The adhesion noise is extracted from the difference (ΔS_V) between total S_V and S_V of the bare sensor, assuming that the two noise sources are independent [5]. We identify the frequency range with a flat adhesion noise spectrum (Fig. 2B black and grey trace), which is indicative of a purely resistive cleft [4]. For type I MEA this ranges from low frequencies to about 5 kHz with an amplitude of 0.009 $\mu V^2/Hz$. Using the equation

$$R_{cleft} = \Delta S_V/(4k_BT) \quad (1)$$

with a thermal energy k_BT [5] at incubation temperature a cleft resistance of 0.52 MΩ is estimated. This value is smaller than reported previously for single neurons [4] but within the expected range. For higher frequencies the spectral power density S_V drops. The decay of S_V at frequencies higher than 5 kHz needs to be investigated in future work. For CMOS MEA type II the spectrum of ΔS_V is flat (i.e., resistive). At frequencies above 5 kHz ΔS_V is 0.045 $\mu V^2/Hz$. This value for ΔS_V (CMOS MEA II) is about 5 times higher than calculated for CMOS MEA Type I.

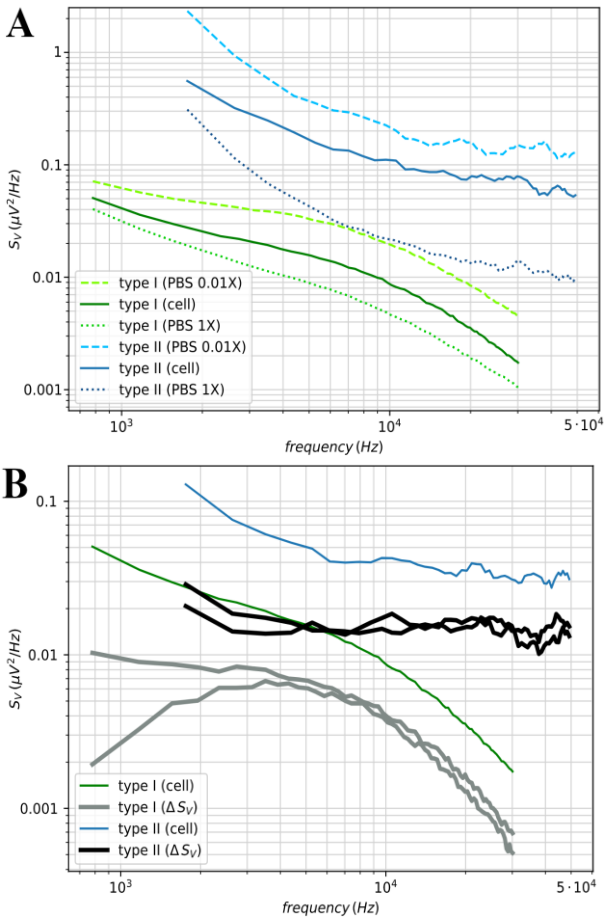

Fig. 2 (A): Spectral power density of the voltage noise at the electrolyte-oxide interface of the MEAs for different PBS concentrations (1X, 0.01X) and with adherent cells as a function of frequency. An electrode covered by a cell (continuous line) results in higher S_V compared to PBS (1X) recordings (dotted traces). A low PBS concentration (0.01X) results in an elevated S_V (dashed traces). Graphs for the electrode from type I CMOS MEA are shown in green, for type II CMOS MEA in blue. (B): Adhesion noise spectra (ΔS_V) for type I MEA and type II MEA.

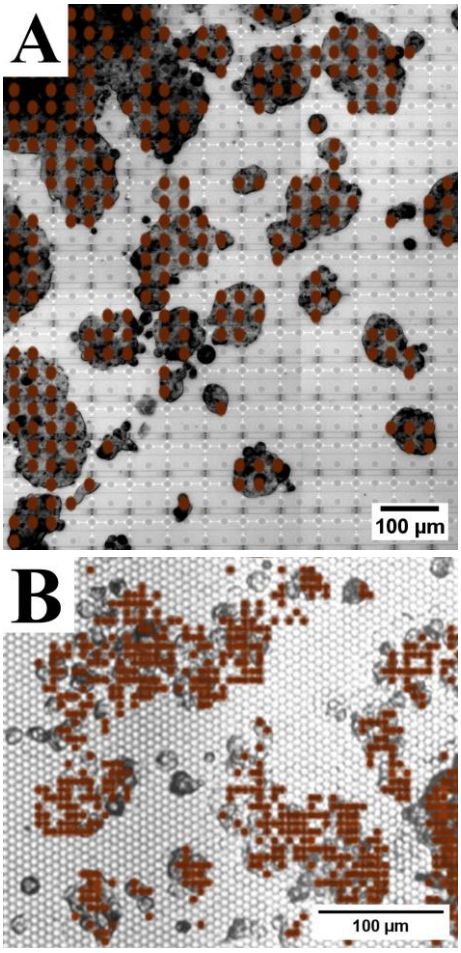

Fig. 3: Identification of adherent cells by adhesion voltage noise (S_V evaluated up to 5 kHz bandwidth for MEA type I and up to 10 kHz bandwidth for MEA type II). Electrical imaging of HT-29 cells is largely in accordance with brightfield microscopic imaging. (A) HT-29 cells on MEA type I, (B) HT-29 cells on MEA type II.

The ratio agrees with the expected ratio based on the formula derived from [6]:

$$S_V^{MEA\ II}/S_V^{MEA\ I} = 1+4\ ln(a_I/a_{II}) \qquad (2)$$

The estimated cleft resistance R_{cleft} of 2.6 MΩ agrees with the value reported for single neurons [4].

Label-free identification of adherent cells is reproducibly accomplished using the spectral power density S_V of the adhesion noise. The adhesion noise spectrum ΔS_V from different sensor sites with adherent cells consistently exhibits homogeneous curves. We define certain sensors that detect adherent cells on each CMOS MEA type as "positive sensors" based on their value S_V, which must exceed the sum of ΔS_V (the change in S_V, Fig. 2B black and grey traces) and the values of S_V of bare sensors (i.e., sensors exposed to the electrolyte). With this criterion, we identify sensors with adherent cells.

For the type I MEA (evaluated using a bandwidth up to 5 kHz), a scatter plot of electrically identified cells (red dots) is overlaid with a brightfield microscopic image (Fig. 3A). A high percentage (85 %) of > 1000 positive sensors indeed show adherent cells. However, there are cells which are not detected (i.e., in the upper left part in Fig. 3A), potentially due to poor cell attachment. A similar procedure is performed with type II CMOS MEA (evaluated at 10 kHz bandwidth, Fig. 3B). The label-free identification indicates a high correspondence (80 %) between label-free detected cells and microscopically identified cells. Undetected small structures on the sensor surface indicate dead cells.

IV. Discussion

We demonstrated how to use CMOS MEAs for label-free identification of adherent, nonelectrogenic cells. Our approach does not require any external stimulation nor perturbation of cells, e.g., staining with a dye or contacting with a pipette. The adhesion voltage noise qualitatively matches values reported earlier for larger neurons [4-6].

From a methodological perspective future work is aimed to improve the identification accuracy and to clarify the health status of nonidentified cells on the sensor sites [14,15]. On the theoretical part a quantitative understanding of the adhesion noise for small cells is required.

Acknowledgment

We thank Mai Thu Bui for assistance with cell culture.

REFERENCES

[1] R. Thewes et al., "Neural tissue and brain interfacing CMOS devices — An introduction to state-of-the-art, current and future challenges," 2016 IEEE International Symposium on Circuits and Systems (ISCAS), Montreal, QC, Canada, 2016, pp. 1826-1829, doi: 10.1109/ISCAS.2016.7538925.

[2] A. Hierlemann, U. Frey, S. Hafizovic and F. Heer, "Growing Cells Atop Microelectronic Chips: Interfacing Electrogenic Cells In Vitro With CMOS-Based Microelectrode Arrays," in Proceedings of the IEEE, vol. 99, no. 2, pp. 252-284, Feb. 2011, doi: 10.1109/JPROC.2010.2066532.

[3] G. Zeck, F. Jetter, L. Channappa, G. Bertotti and R. Thewes, "Electrical imaging: Investigating cellular function at high resolution," Advanced Biosystems, vol. 1, iss. 11, Oct. 2017, doi: 10.1002/adbi.201700107.

[4] M. Voelker and P. Fromherz, "Nyquist noise of cell adhesion detected in a neuron-silicon transistor," Physical Review Letters, vol. 96, iss. 22, June 2006, doi: 10.1103/physrevlett.96.228102.

[5] R. Zeitler, P. Fromherz and G. Zeck, "Extracellular voltage noise probes the interface between Retina and Silicon Chip," Applied Physics Letters, vol. 99, iss. 26, Dec. 2011, doi: 10.1063/1.3672224.

[6] R. Zeitler and P. Fromherz, "The thermal voltage fluctuations in the planar core-coat conductor of a neuron-semiconductor interface," Langmuir, vol. 29, iss. 20, pp. 6084-6090, Apr. 2013, doi: 10.1021/la4002169.

[7] P. R. Rocha, et al., "Electrochemical noise and impedance of AU electrode/electrolyte interfaces enabling extracellular detection of glioma cell populations," Scientific Reports, vol. 6, iss. 1, Oct. 2016, doi: 10.1038/srep34843.

[8] Laborde, C. et al., "Real-time imaging of microparticles and living cells with CMOS nanocapacitor arrays," Nature Nanotechnology, vol. 10, iss. 9, pp. 791–795, Aug. 2015, doi: 10.1038/nnano.2015.163.

[9] T. Lausen et al., "A Low-Noise Ex-Vivo CMOS MEA with 4k Recording Sites, 4k Recording Channels, and 1k Stimulation Sites," 2022 IEEE Biomedical Circuits and Systems Conference (BioCAS), Taipei, Taiwan, 2022, pp. 524-528, doi: 10.1109/BioCAS54905.2022.9948664.

[10] Corna, A., Ramesh, P., Jetter, F., Lee, M.-J., Macke, J. H. and Zeck, G. "Discrimination of simple objects decoded from the output of retinal ganglion cells upon sinusoidal electrical stimulation," Journal of Neural Engineering, vol. 18, iss. 4, June 2021, doi: 10.1088/1741-2552/ac0679.

[11] E. A. Vallicelli et al., "Neural spikes digital detector/sorting on FPGA," 2017 IEEE Biomedical Circuits and Systems Conference (BioCAS), Turin, Italy, 2017, pp. 1-4, doi: 10.1109/BIOCAS.2017.8325077.

[12] Pauli Virtanen, et al. "SciPy 1.0: Fundamental Algorithms for Scientific Computing in Python," Nature Methods, vol. 17, iss. 3, pp. 261-272, Feb. 2020, doi: 10.1038/s41592-019-0686-2.

[13] E. A. Vallicelli et al., "Real-time digital implementation of a principal component analysis algorithm for neurons spike detection," 2018 International Conference on IC Design & Technology (ICICDT), Otranto, Italy, 2018, pp. 33-36, doi: 10.1109/ICICDT.2018.8399749.

[14] J. Abbott, et al., "Multi-parametric functional imaging of Cell Cultures and tissues with a CMOS microelectrode array," Lab on a Chip, vol. 22, iss. 7, pp. 1286–1296, doi: 10.1039/d1lc00878a.

[15] I. L. Jones, P. Livi, M. K. Lewandowska, M. Fiscella, B. Roscic and A. Hierlemann, "The potential of microelectrode arrays and microelectronics for Biomedical Research and Diagnostics," Analytical and Bioanalytical Chemistry, vol. 399, iss. 7, pp. 2313-2329, doi: 10.1007/s00216-010-3968-1.